Georg-August-Universität

Göttingen

Calibration of model and discretization parameters for turbulent channel flow

Zhang, X.Q., Knopp, T., Lube, G.

Nr. 2007-26

Preprint-Serie des
Instituts für Numerische und Angewandte Mathematik
Lotzestr. 16-18
D - 37083 Göttingen

Calibration of Model and Discretization Parameters for Turbulent Channel Flow

X.Q. Zhang, T. Knopp, and G. Lube

Abstract The simulation of turbulent incompressible flow in a plane channel is addressed. For $Re_\tau = 395$, discretization and model parameters of LES and DES models are calibrated using a DNS data basis. For higher Re_τ, a non-zonal hybrid method combines the calibrated LES model with wall functions as a near-wall model.

1 Basic mathematical model and discretization

Consider the non-stationary, incompressible Navier-Stokes model

$$\partial_t \mathbf{u} - \nabla \cdot (2\nu \mathbb{S}(\mathbf{u})) + \nabla \cdot (\mathbf{u} \otimes \mathbf{u}) + \nabla p = \mathbf{f} \qquad \text{in } \Omega \times (0,T] \tag{1}$$

$$\nabla \cdot \mathbf{u} = 0 \qquad \text{in } \Omega \times (0,T] \tag{2}$$

for velocity $\mathbf{u}$ and pressure p in a bounded, polyhedral domain $\Omega \subset \mathbb{R}^3$ together with boundary and initial conditions. $\mathbb{S}(\mathbf{u}) = \frac{1}{2}(\nabla \mathbf{u} + \nabla \mathbf{u}^T)$ is the rate of strain tensor.

For the numerical simulation of (1)-(2), the DLR Theta code is used. The spatial discretization is based on a finite volume scheme on unstructured collocated grids. Different upwind schemes (linear upwind scheme (LUDS), quadratic upwind scheme (QUDS)) and the central differencing scheme (CDS) are implemented for the approximation of the convective fluxes. Diffusive fluxes are discretized with the CDS. The interpolation scheme by Rhie and Chow [8] is applied in order to avoid spurious pressure oscillations. The time discretization is performed using the A-stable BDF(2) scheme. The incremental variant of the projection method is used to

X.Q. Zhang/ G. Lube
Math. Department, Georg-August-University Göttingen, Lotzestrasse 16-18, D-37083 Göttingen, Germany, e-mail: xiazhang/lube@math.uni-goettingen.de

T. Knopp
Institute of Aerodynamics and Flow Technology, German Aerospace Center (DLR) Göttingen, Bunsenstrasse 10, D-37073 Göttingen, Germany, e-mail: Tobias.Knopp@dlr.de

split the calculation of velocity and pressure within each time step. For a review of semidiscrete error estimates for the time-dependent Stokes problem see [3].

Of special interest here is the wall treatment. In the code, the wall node is shifted to the center of the control volume adjacent to the wall. Denote Γ_{w} the wall and Γ_δ an artificial inner boundary containing the shifted nodes at wall distance y_δ. Then, as a boundary condition on Γ_{w}, the wall-shear stress τ_{w} is prescribed instead of no-slip

$$\mathbf{u}\cdot\mathbf{n}=0, \quad (\mathbb{I}-\mathbf{n}\otimes\mathbf{n})2\nu\mathbb{S}(\mathbf{u})\mathbf{n}=-\tau_{\mathrm{w}}\mathbf{u}_{\mathrm{t},\delta} \quad \text{on} \quad \Gamma_{\mathrm{w}} . \tag{3}$$

with $\mathbb{I}-\mathbf{n}\otimes\mathbf{n}$ being the projection operator onto the tangential space of Γ_{w}, unit velocity vector in wall-parallel direction $\mathbf{u}_{\mathrm{t},\delta}=\mathbf{v}_{\mathrm{t},\delta}/|\mathbf{v}_{\mathrm{t},\delta}|$ and

$$\tau_{\mathrm{w}}=\nu\nabla u_\delta\cdot\mathbf{n}\,, \quad \text{where} \quad u_\delta \;=\; |\mathbf{v}_{\mathrm{t},\delta}|\,, \quad \mathbf{v}_{\mathrm{t},\delta}=(\mathbb{I}-\mathbf{n}\otimes\mathbf{n})\,\mathbf{u}|_{\Gamma_\delta} . \tag{4}$$

2 Turbulence modeling using LES type models

In LES, a scale separation operator subdivides the scales into filtered scales and unresolved scales. Only the filtered scales are solved and the unresolved scales are modeled by a sub-grid stress term of the so-called eddy-viscosity ν_{t}.

Smagorinsky model: In this classical LES model, the eddy-viscosity is given by $\nu_{\mathrm{t}}=(C_S\Delta)^2|\mathbb{S}|$ with $|\mathbb{S}|=(2\mathbb{S}:\mathbb{S})^{1/2}$. The model constant to be calibrated is C_S. The filter width is $\Delta=nh_{\mathrm{c}},\ n=1,2,\ldots$, with $h_{\mathrm{c}}=(\Delta x\Delta y\Delta z)^{1/3}$, where $\Delta x,\Delta y,\Delta z$ denote the grid spacing in x-, y-, and z-direction respectively.

Near solid walls, the turbulent viscosity ν_{t} is multiplied with the van Driest damping function $D(y^+)$. For $\mathbf{x}\in\Omega$, denote $\mathbf{x}_{\mathrm{w}}=\mathbf{x}_{\mathrm{w}}(\mathbf{x})\in\Gamma_{\mathrm{w}}$ the corresponding nearest wall point with distance d from $\mathbf{x}$. Then $D(y^+)=(1-\exp(-y^+/A^+))^2$ with $A^+=26$ where $y^+=yu_\tau/\nu$ is the wall-distance of $\mathbf{x}$ from $\mathbf{x}_{\mathrm{w}}$ in viscous units with $y=\mathrm{dist}(\mathbf{x},\mathbf{x}_w(\mathbf{x}))\equiv d$ and $u_\tau=u_\tau|_{\mathbf{x}_{\mathrm{w}}}=\sqrt{\tau_{\mathrm{w}}}$.

Due to its non-local character the van Driest damping is not very suitable for unstructured methods or if parallelization is used A modified definition of Δ by [11] uses $\Delta=\min(\max(C_{\mathrm{w}}d,C_{\mathrm{w}}\Delta_{\max},\Delta_{\mathrm{wn}}),\ \Delta_{\max})$ where $\Delta_{\max}=\max\{\Delta x,\Delta y,\Delta z\}$ with Δ_{wn} denoting the spacing in wall-normal direction. C_{w} is a calibration parameter.

Detached-eddy simulation model: Detached-eddy simulation (DES) is a single non-zonal hybrid RANS-LES method [10] based on the one-equation RANS model by Spalart & Allmaras [9] which computes the eddy viscosity $\nu_{\mathrm{t}}=f_{v1}\tilde{\nu}$ from the auxiliary viscosity $\tilde{\nu}$ using a near-wall damping function $f_{v1}=\chi^3/(\chi^3+c_{v1}^3)$ with $\chi=\tilde{\nu}/\nu$ which involves only local variables. Here $\tilde{\nu}$ solves the transport equation

$$\partial_t\tilde{\nu}+\mathbf{u}\cdot\nabla\tilde{\nu}-\nabla\cdot\left(\frac{\nu+\tilde{\nu}}{\sigma}\nabla\tilde{\nu}\right)-\frac{c_{b2}}{\sigma}(\nabla\tilde{\nu})^2 \;=\; c_{b1}\tilde{S}\tilde{\nu}-c_{w1}f_w(\frac{\tilde{\nu}}{d})^2$$

with $\tilde{S}=|\Omega|+\tilde{\nu}/(\kappa^2d^2)f_{v2}$, $|\Omega|=(2\Omega(\mathbf{u}):\Omega(\mathbf{u}))^{1/2}$, and $\Omega(\mathbf{u})=(\nabla\mathbf{u}-(\nabla\mathbf{u})^T)/2$. The functions f_w and f_{v2} and constants σ, c_{b2}, c_{b1}, c_{w1} are given in [9].

In the SA-DES model, d is replaced with $\tilde{d} = \min(d , C_{DES}\Delta_{\max})$. The model constant to be calibrated is C_{DES}.

Near-wall treatment for LES: Wall-functions are used to bridge the near-wall region at high Reynolds numbers. The wall shear stress τ_{w} can be computed from (4) only if $y_\delta^+ < 3$. For larger y_δ^+, $\tau_{\mathrm{w}} = u_\tau^2$ is computed from friction velocity u_τ: The universal velocity profile of RANS-type by Reichardt is matched at the shifted node y_δ with the instantaneous LES solution u_δ

$$\frac{u_\delta}{u_\tau} = F\left(\frac{y_\delta u_\tau}{\nu}\right) , \quad F(y^+) \equiv \frac{\ln(1+0.4y^+)}{\kappa} + 7.8\left(1 - e^{-\frac{y^+}{11.0}} - \frac{y^+}{11.0}e^{-\frac{y^+}{3.0}}\right). \quad (5)$$

Equation (5) is solved for u_τ with Newton's method.

We remark that (5) is an approximative solution of the boundary layer equation in wall-normal direction neglecting convective term and pressure gradient: For each $\mathbf{x}_{\mathrm{w}} \in \Gamma_{\mathrm{w}}$ and given u_δ seek the wall-parallel velocity $u^{\mathrm{RANS}}(y)$ such that

$$\partial_y\Big((\nu + \nu_{\mathrm{t}}^{\mathrm{RANS}})\partial_y u^{\mathrm{RANS}}\Big) = 0 \quad \text{in} \qquad \{ \mathbf{x}_{\mathrm{w}} - y\mathbf{n} \mid y \in (0, y_\delta)\} \quad (6)$$

$$u^{\mathrm{RANS}}(0) = 0 , \qquad u^{\mathrm{RANS}}(y_\delta) = u_\delta . \quad (7)$$

3 Calibration for decaying isotropic turbulence

Framework: It is desirable to treat the calibration problem of basic turbulence models within the framework of optimization problems. Consider the abstract equation

$$A(q,u) = f \quad \text{in} \quad \Omega. \quad (8)$$

(here: quasi-stationary turbulent Navier-Stokes model) for the state variable u (here: velocity/pressure) in a Hilbert space $V \subseteq [H^1(\Omega)]^3 \times L^2(\Omega)$ with the parameter vector q (here: model and grid parameter) in the control space $Q := \mathbb{R}^{n_p}$. Let $C : V \to Z$ be a linear observation operator mapping u into the space of measurements $Z := \mathbb{R}^{n_m}$ with $n_m \geq n_p$. Then q is calculated from the constrained optimization problem

$$\text{Minimize} \qquad J(q,u) := \|C(u) - \hat{C}\|_Z^2/2 \quad (9)$$

with the cost functional $J : Q \times V \to \mathbb{R}$ under constraint (8) and using measurements $\hat{C} \in Z$. Assume the existence of a unique solution to (8)-(9) and of an open set $Q_0 \subset Q$ containing the optimal solution. Using the solution operator $S : Q_0 \to V$, one defines via $u = S(q)$ the reduced cost functional $j : Q_0 \to \mathbb{R}$ by $j(q) = J(q, S(q))$. The reduced observation operator $c(q) := C(S(q))$ leads to an unconstrained problem

$$\text{Minimize} \quad j(q) = \|c(q) - \hat{C}\|_Z^2/2, \qquad q \in Q_0. \quad (10)$$

An efficient framework to the solution of the necessary optimality condition $j'(q) = 0$ of (10) provides the adjoint approach, see [4] for a review. The approach can be generalized to time-dependent problems. This makes the optimization problem and solution techniques much more expensive, although sophisticated tools such as a-posteriori based optimization can reduce the costs, e.g. [1].

Seemingly, this approach has not been applied to parameter identification for turbulent flows yet. Main problems occur from the nonlinearity of turbulence models and the simulation over long time intervals to reach a statistically steady solution. Hence, a simpler approach to (10) is applied. As a basic step, a series of numerical simulations for a given flow provide look-up tables for the cost functional depending on relevant parameters as a basis for further systematic considering. In some cases, a Newton type method is feasible to determine optimized parameters.

Application to DIT: The problem of decaying isotropic turbulence (DIT) mimics the experiment by [2] at Taylor microscale Reynolds number $Re_\lambda \sim 150$. We choose a cubic box domain $\Omega = (0,2\pi)^3$ and an equidistant mesh with N^3 nodes. As initial condition, we use a divergence-free velocity field with energy spectrum $E(k)|_{t=0}$ ($k = |\mathbf{k}|$, $1 \le k \le M$, $M = N/2-1$) given by data in [2] which can be computed as

$$\mathbf{u}(\mathbf{x})|_{t=0} \;=\; \sum_{\substack{k_1=0\\ |\mathbf{k}|\le k_{\max}}}^{M} \sum_{k_2,k_3=-M}^{M} \Big(\frac{E(k)|_{t=0}}{S_k}\Big)^{1/2} 2\Big(\mathbb{I} - \frac{\mathbf{k}\otimes\mathbf{k}}{|\mathbf{k}|^2}\Big)\gamma(\mathbf{k})\cos(\mathbf{k}\cdot\mathbf{x}+\Theta(\mathbf{k})). \quad (11)$$

The components of $\gamma(\mathbf{k})$ are real random numbers with Gaussian distribution in $[0,1]$, S_k is the number of wave-vectors $\mathbf{k}$ with $k-1/2 \le |\mathbf{k}| \le k+1/2$ and $\Theta(\mathbf{k})$ is a random phase with uniform distribution in $0 \le \Theta \le 2\pi$.

The second-order statistics of interest is the energy spectrum

$$E(k,t) \;=\; \sum_{k-1/2<|\mathbf{q}|\le k+1/2} \frac{1}{2}\hat{\mathbf{u}}(\mathbf{q},t)\cdot\hat{\mathbf{u}}^*(\mathbf{q},t), \qquad k = 1,2,\ldots,M, \qquad (12)$$

where $\hat{\mathbf{u}}^*$ is the complex conjugated of $\hat{\mathbf{u}}$. $\hat{\mathbf{u}}$ is the discrete Fourier transform of $\mathbf{u}$

$$\hat{\mathbf{u}}(\mathbf{k}) \;=\; \frac{1}{N^3}\Big(\sum_{x_1,x_2,x_3=0}^{N-1}\mathbf{u}(\mathbf{x})\cos(-\mathbf{k}\cdot\mathbf{x}) + i\sum_{x_1,x_2,x_3=0}^{N-1}\mathbf{u}(\mathbf{x})\sin(-\mathbf{k}\cdot\mathbf{x})\Big). \qquad (13)$$

Then we consider the error functional

$$J(C) \;=\; \Big(\;\sum_{i=1}^{M}\Big[\big(E(k_i,C)-E_{\exp}(k_i)\big)^2_{t=0.87} \;+\; \big(E(k_i,C)-E_{\exp}(k_i)\big)^2_{t=2.0}\Big]\;\Big)^{1/2}.$$

The results in [12] for the spatial discretizations show that CDS is suitable to resolve the large wave-number part of the spectrum, whereas the upwind schemes produce excessive damping at high wave-numbers. Combining QUDS with a skew-symmetric formulation (QUDS_sk) for the convective fluxes gives some improvement. Fig. 1 (left) shows the dependence of the cost functional on the constant C_S for the Smagorinsky model (SMG) and $N = 64$. A Newton-type method (based on numerical differentiation) delivers a minimum with $C_S = 0.094$ for CDS and

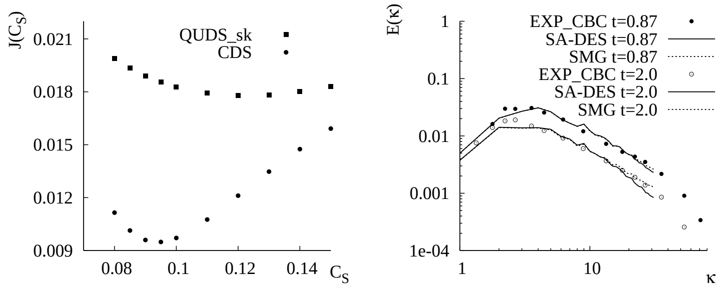

Fig. 1 Left: Calibration of Smagorinsky constant C_S for DIT. Right: Energy spectrum with optimized model constants of Smagorinsky model and of SA-DES model for CDS scheme.

$C_S = 0.123$ for QUDS_sk. For the SA-DES model, a similar Newton-type approach yields a minimum of $J(C)$ for $C_{\text{DES}} = 0.67$. In Fig. 1 (right), the corresponding energy spectra for CDS with optimized constants for SMG and SA-DES are shown.

4 Parameter calibration for channel flow

Consider now the benchmark problem of fully developed turbulent channel flow in the domain $\Omega = (0,2\pi) \times (0,2) \times (0,\pi)$. Periodic boundary conditions in streamwise x-direction, a no-slip condition for the walls in y-direction and symmetry planes in the spanwise z-direction are imposed. We consider a moderate Reynolds number $Re_\tau = u_\tau H/\nu = 395$ with channel half width $H = 1$, for which DNS data are available [6]. In order to achieve a constant mass flux, the streamwise forcing term is adjusted dynamically by taking into account the time step size δt_n and the bulk velocity from the DNS data and the bulk velocity at the present time t_n

$$\mathbf{f} \;=\; \tau_{\text{w}} \mathbf{e}_x \;+\; (\delta t_n)^{-1} (U_{\text{bulk,DNS}} - U_{\text{bulk}}(t_n)) \mathbf{e}_x \,, \quad U_{\text{bulk}} = H^{-1} \int_0^H u(y) \mathrm{d}y \tag{14}$$

where $\mathbf{e}_x$ denotes the unit-vector in x-direction. As initial condition we use a randomly perturbed velocity field $\mathbf{u}|_{t=0} = u_\tau F(yu_\tau/\nu)\mathbf{e}_x + 0.1 U_{\text{bulk}} \psi$ where F is given by (5) and each component of ψ is a random number in $(-1,1)$. The spatial discretization uses $N_x \times N_y \times N_z = 64 \times 64 \times 64$ nodes. The equidistant spacing in x- and z direction corresponds to $\Delta x^+ = \Delta x u_\tau/\nu = 38.8$ and $\Delta z^+ = \Delta z u_\tau/\nu = 19.4$ respectively. The grid in wall-normal direction is stretched using a hyperbolic tangent function $y(j)/H \;=\; \tanh[\gamma(2j/N_y - 1)]/\tanh(\gamma) + \; 1.0, \; j = 0,1,\ldots,N_y - 1$ where $y(j)$ is the coordinate of the jth grid point in y direction providing thus an anisotropic, layer-adapted mesh, see [5]. The parameter γ allows to move the position $y^+(1)$ of the shifted wall node. The time step is chosen as $\delta t^+ \equiv \delta t u_\tau^2/\nu = 0.4$.

After reaching a statistically steady solution, first-order and second order statistics are computed. Denote $\langle \cdot \rangle$ the averaging operator over the two homogeneous

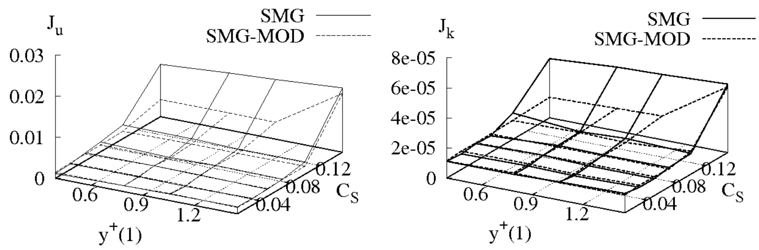

Fig. 2 Cost functionals for channel flow $Re_\tau = 395$, Left: mean velocity. Right: kinetic energy.

directions and in time. The quantities of interest are the mean velocity $U = \langle u \rangle$, the turbulent kinetic energy $k = \frac{1}{2}\langle (u - \langle u \rangle)^2 \rangle$ and its normalized variants $U^+ = \frac{U}{u_\tau}$ and $k^+ = \frac{k}{u_\tau^2}$. The L^2-error functional of the LES results compared to the DNS data is

$$J_u(y^+(1), C) = \Big(\sum_{i=0}^{N_y} (U_i(y^+(1), C) - U_{i,\mathrm{DNS}})^2 \Delta y_i \Big)^{1/2} \tag{15}$$

for the mean velocity (and similarly for kinetic energy J_k) with $\phi_i = \phi(y(i))$ and the spacing Δy_i in y-direction of cell i.

In Fig. 2, the dependence of the cost functionals J_u and J_k on C_S and $y^+(1)$ is shown for the Smagorinsky model. The result is robustness w.r.t. $C_S \in [0, 0.12]$ and $y^+(1) \in [0.5, 1.5]$. This means that a Newton-type approach to parameter calibration will not find local minima. In particular, the DIT-optimized value of C_S but also $C_S = 0$ (i.e., no turbulence model) are reasonable. The latter simulation can be seen as underresolved DNS on a layer-adapted mesh.

Reasonable results for the first and second order statistics are presented in Fig. 3 for the calibrated modified Smagorinsky model and the SA-DES model. The SA-DES model gives even better results and allows to avoid a damping of ν_t.

Channel flow at higher Re_τ: Now, the goal is to simulate turbulent channel flow at higher Reynolds number $Re_\tau = 4800$ using the calibrated model constants. A resolution of the wall layer regions (as for $Re_\tau = 395$) with a standard LES model is not feasible (on a single processor) due to the much finer mesh in all spatial directions and in time.

As DES-type approaches are still relatively expensive, the modified Smagorinsky LES model (WSMAG) and the SA-DES model (WSADES) are used with wall functions. This reduces the computing time by an order of magnitude due to the saving in grid points in wall-normal direction and due to the much larger time steps.

The results for the WSADES approach are given in Fig. 4. The original DES concept for coupling the RANS and LES regions gives two logarithmic layers, see [7]. The lower layer is the modeled log layer of the RANS model, while the upper layer is the resolved log-layer of the LES model. This causes a significant error in u_τ. This is subject to present and future research and will be presented elsewhere.

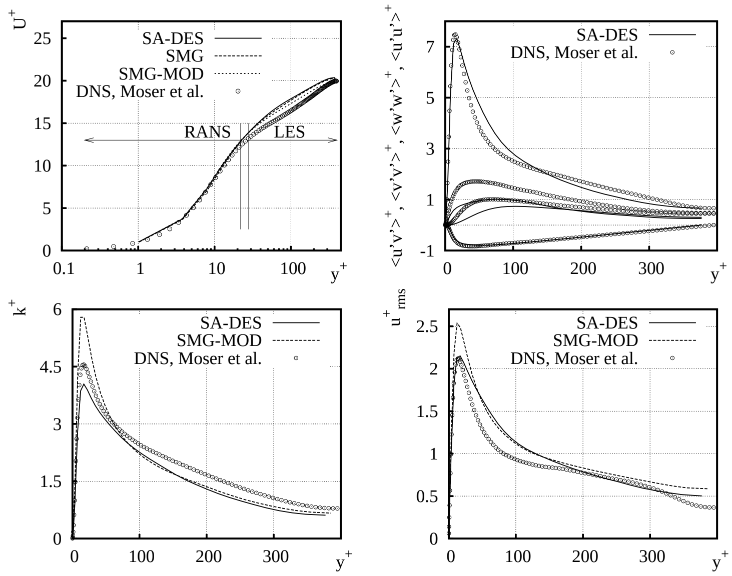

Fig. 3 Channel flow $Re_\tau = 395$ for modified Smagorinsky and SA-DES model: Upper left: Mean velocity U^+. Upper right: Fluctuations. Bottom left: Kinetic energy k^+. Bottom right: u^+_{rms}.

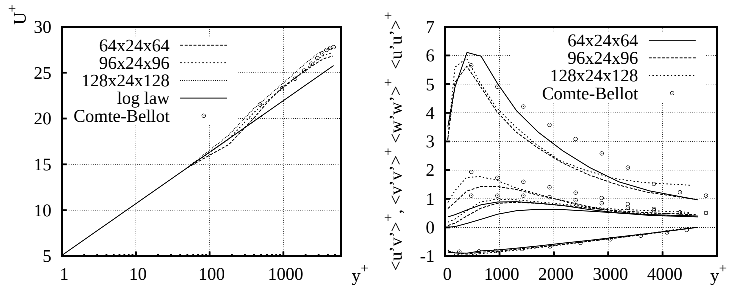

Fig. 4 SA-DES model with near-wall modeling (WSADES) for channel flow $Re_\tau = 4800$.

5 Summary. Conclusions

A strategy for calibration of model and discretization parameters of LES and DES within the framework of optimization techniques was presented. We use the DLR Theta code, which is an industrial RANS solver. Precurser studies on the benchmark problems of decaying isotropic turbulence and of turbulent channel flow at $Re_\tau = 395$ show that the central difference scheme (CDS) for the convective term is clearly superior to upwind schemes. Moreover it can be seen that second order accurate time discretization is necessary for proper calculation of second order statistics for turbulent channel flow.

A calibration of model and grid parameters was performed based on least-squares cost functionals for first and second order flow statistics. Best results for channel flow at $Re_\tau = 395$ are found for the calibrated SA-DES model which also avoids van Driest damping. Finally the optimized parameters are used for a simulation of turbulent channel flow at $Re_\tau = 4800$. A proper near-wall resolution is very expensive at such Reynolds numbers. Therefore LES and DES in combination with near-wall modeling based on wall functions are used and reasonable results are obtained.

Future work will be on turbulent channel flow at high Reynolds numbers with focus on more sophisticated methods for coupling hybrid wall-functions with LES. Another task will be on continuation of the wall-resolved LES for the flow over a backward facing step.

Acknowledgements The first author gratefully acknowledges financial support by the Deutsche Forschungsgemeinschaft (DFG) via GK 1023. This work benefited from the discussions of the second author within the DESider project (Detached Eddy Simulation for Industrial Aerodynamics) funded by the European Union and administrated by the CEC, Research Directorate-General, Growth Programme, under Contract No. AST3-CT-2003-502842. Finally we thank Dr. R. Kessler for valuable discussions and support with the DLR Theta code.

References

1. Becker, R., Braack, M., Vexler, B.: Parameter identification for chemical models in combustion problems. Applied Numerical Mathematics **54(3-4)**, 519–536 (2005)
2. Comte-Bellot, G., Corrsin, S.: Simple eulerian time correlation of full- and narrow-band velocity signals in grid-generated, 'isotropic' turbulence. Journal of Fluid Mechanics **48(2)**, 273–337 (1971)
3. Guermond, J., Minev, P., Shen, P.: An overview of projection methods for incompressible flows. Computer Methods in Applied Mechanics and Engineering **196**, 6011–6045 (2006)
4. Johansson, H., Runesson, K., Larsson, F.: Parameter identification with sensitivity assessment and error computation. GAMM-Mitteilungen **30(2)**, 430–457 (2007)
5. Morinishi, Y., Vasilyev, D.: A recommended modification to the dynamic two-parameter mixed subgrid scale model for large eddy simulation of wall bounded turbulent flow. Physics of Fluids **13**, 3400–3410 (2001)
6. Moser, R., Kim, J., Mansour, N.: Direct numerical simulation of turbulent channel flow up to $Re_\tau = 590$. Physics of Fluids **11**, 943–946 (1999)
7. Nikitin, N.V., Nicoud, F., Wasistho, B., Squires, K.D., Spalart, P.R.: An approach to wall modeling in large-eddy simulation. Physics of Fluids **12(7)**, 1629–1632 (2000)
8. Rhie, C.M., Chow, W.L..: Numerical study of the turbulent flow past an airfoil with trailing edge separation. AIAA Journal **21**, 1525–1532 (1983)
9. Spalart, P.R., Allmaras, S.R.: A one-equation turbulence model for aerodynamics flows. AIAA Paper 1992-0439 (1992)
10. Spalart, P.R., Jou, W.H., Strelets, M., Allmaras, S.R.: Comments on the feasibility of les for wings, and on a hybrid rans/les approach. August, 1997, In: Advances in DNS/LES, edited by C. Liu and Z. Liu (Greyden, Columbus, OH, 1997) (1997)
11. Travin, A., Shur, M., Spalart, P.R., Strelets, M.: Improvement of delayed detached-eddy simulation for les with wall modelling. In: Proceedings of the European Conference on Computational Fluid Dynamics (ECCOMAS CFD 2006) (2006)
12. Zhang, X.Q.: Identification of model and grid parameters for incompressible turbulent flows. Ph.D. thesis, University Göttingen (2007)

Institut für Numerische und Angewandte Mathematik
Universität Göttingen
Lotzestr. 16-18
D - 37083 Göttingen

Telefon: 0551/394512
Telefax: 0551/393944

Email: trapp@math.uni-goettingen.de URL: http://www.num.math.uni-goettingen.de

Verzeichnis der erschienenen Preprints 2007:

2007-01	P. Serranho	A hybrid method for inverse scattering for sound-soft obstacles in 3D
2007-02	G. Matthies, G. Lube	On streamline-diffusion methods for inf-sup stable discretisations of the generalised Oseen Problem
2007-03	A. Schöbel	Capacity constraints in delay management
2007-04	J. Brimberg, H. Juel, A. Schöbel	Locating a minisum circle on the plane
2007-05	C. Conte, A. Schöbel	Identifying dependencies among delays
2007-06	D.S. Gilliam, T. Hohage, X. Ji, F. Ruymgaart	The Frechet-derivative of an analytic function of a bounded operator with some applications
2007-07	T. Hohage, M. Pricop	Nonlinear Tikhonov regularization in Hilbert scales for inverse boundary value problems with random noise
2007-08	C.J.S. Alves, R. Kress, A.L. Silvestre	Integral equations for an inverse boundary value problem for the two-dimensional Stokes equations
2007-09	A. Ginkel, A. Schöbel	To wait or not to wait? The bicriteria delay management problem in public transportation
2007-10	O. Ivanyshyn, R. Kress	Inverse scattering for planar cracks via nonlinear integral equations
2007-11	F. Delbary, K. Erhard, R. Kress, R. Potthast, J. Schulz	Inverse electromagnetic scattering in a two-layered medium with an application to mine detection
2007-12	M. Pieper	Vector hyperinterpolation on the sphere
2007-13	M. Pieper	Nonlinear integral equations for an inverse electromagnetic scattering problem
2007-14	I. Akduman, R. Kress, N. Tezel, F. Yaman	A second order Newton method for sound soft inverse obstacle scattering

2007-15	M. Schachtebeck, A. Schöbel	Algorithms for delay management with capacity constraints
2007-16	R. Kress, F. Yaman, A. Yapar, I. Akduman	Inverse scattering for an impedance cylinder buried in a dielectric cylinder
2007-17	T. Hohage, L. Nannen	Hardy space infinite elements for scattering and resonance problems
2007-18	De Marchi, Stefano, Schaback, R.	Stability of kernel-based interpolation
2007-19	Schaback, R.	Solving the Laplace Equation by Meshless Collocation Using Harmonic Kernels
2007.20	Schaback, R.	Adaptive numerical solution of MFS systems
2007.21	Schaback, R.	A Posteriori Error Estimates for Meshless Methods
2007.22	Lee, C.-F., Ling, L., Schaback, R.	On Convergent Numerical Algorithms for Unsymmetric Collocation
2007.23	Ling, L., Schaback, R.	Stable and Convergent Unsymmetric Meshless Collocation Methods
2007-24	C. Liebchen, M. Schachtebeck, A. Schöbel, S. Stiller, A. Prigge	Computing Delay Resistant Railway Timetables
2007-25	G. Lube, T. Knopp, G. Rapin, R. Gritzki, M. Rösler	Application of stabilized finite element methods to indoor air flow simulations
2007-26	X.Q. Zhang, T. Knopp, G. Lube	Calibration of model and discretization parameters for turbulent channel flow